GEOPHYSICAL RESEARCH LETTERS, VOL. 33, L14402, doi:10.1029/2006GL026816, 2006

Simulating heat transport of harmonic temperature signals in the Earth's shallow subsurface: Lower-boundary sensitivities

Jason E. Smerdon[1] and Marc Stieglitz[2]

Received 5 May 2006; revised 23 May 2006; accepted 31 May 2006; published 21 July 2006.

[1] We assess the sensitivity of a subsurface thermodynamic model to the depth of its lower-boundary condition. Analytic solutions to the one-dimensional thermal diffusion equation demonstrate that boundary conditions imposed at shallow depths (2–20 m) corrupt the amplitudes and phases of propagating temperature signals. The presented solutions are for: 1) a homogeneous infinite half-space driven by a harmonic surface-temperature boundary condition, and 2) a homogeneous slab with a harmonic surface-temperature boundary condition and zero-flux lower-boundary condition. Differences between the amplitudes and phases of the two solutions range from 0 to almost 100%, depending on depth, frequency and subsurface thermophysical properties. The implications of our results are straightforward: the corruption of subsurface temperatures can affect model assessments of soil microbial activity, vegetation changes, freeze-thaw cycles, and hydrologic dynamics. It is uncertain, however, whether the reported effects will have large enough impacts on land-atmosphere fluxes of water and energy to affect atmospheric simulations. **Citation:** Smerdon, J. E., and M. Stieglitz (2006), Simulating heat transport of harmonic temperature signals in the Earth's shallow subsurface: Lower-boundary sensitivities, *Geophys. Res. Lett.*, *33*, L14402, doi:10.1029/2006GL026816.

1. Introduction

[2] Heat transport in the Earth's subsurface plays an important role in governing water, energy and momentum fluxes at and below the land-surface boundary [e.g., *Hillel*, 1998]. Accurate simulations of subsurface thermodynamics therefore are an essential aspect of land-surface models. The typical thermodynamic component in a land-surface model uses numerical schemes to solve for heat transport along a thermal gradient according to the thermal diffusion equation [e.g., *Schulz et al.*, 1998]. These schemes require a number of choices that influence the accuracy of the simulation. The choices include the number of discretized subsurface layers to use, how thick each subsurface layer should be, which initial conditions to employ, and which lower-boundary condition to impose at the final depth layer. While the choice and depth of the lower boundary condition varies in land-surface models, the common convention is a zero-flux lower-boundary condition, that is, no heat is transported across the bottom boundary, at depths that usually range between 2 and 10 m. Boundary conditions at these depths, however, change the behavior of propagating temperature signals in a way that is not representative of the actual behavior in the Earth's subsurface. Here we explore how the choice and depth of a lower-boundary condition influences the subsequent evolution of subsurface temperatures, given a simple harmonic surface temperature function.

[3] Two studies that have investigated how the depth of the lower-boundary condition affects subsurface temperature evolution are *Lynch-Stieglitz* [1994] and *Sun and Zhang* [2004]. *Lynch-Stieglitz* [1994] investigated the behavior of annual signals in a land-surface model with a zero-flux lower-boundary condition imposed at 2.3 m and noted that the annual signal was attenuated less and phase shifted more with depth than what was expected; that is, the model formulation yielded subsurface temperatures that were warmer in summer and colder in winter, with maximums occurring later in the year, than what was expected in real-world conditions. *Sun and Zhang* [2004] provided an additional investigation of the finite-boundary effect, again focusing on the annual signal. They demonstrated behavior similar to that noted by *Lynch-Stieglitz* [1994] and concluded that land-surface models should place lower boundaries between 6 and 15 m, depending on the thermophysical properties of the modeled subsurface.

[4] Both of the above mentioned studies used numerical land-surface models to elucidate the impact of the lower-boundary condition on simulations of subsurface heat transport and focused only on the annual signal. We take an alternative approach to this problem and employ analytic solutions of the one-dimensional thermal diffusion equation. This approach allows a more general and transparent understanding of how the depth of the lower-boundary condition impacts simulations of heat transport across a wide range of frequencies.

2. Background

[5] We employ analytic solutions of the one-dimensional thermal diffusion equation to investigate the influence of a zero-flux lower-boundary condition on calculations of subsurface heat transport. The solutions are for two scenarios: 1) a sinusoidal temperature boundary condition at the surface of an infinite half space, and 2) a sinusoidal temperature boundary condition at the surface of a slab with a zero-flux boundary condition at a finite depth. The first scenario is representative of real-world conditions, the second represents the modeled conditions in many land-surface models.

[6] Assuming a homogeneous subsurface, no internal heat production and a sinusoidal surface temperature

[1]Lamont-Doherty Earth Observatory, Columbia University, Palisades, New York, USA.
[2]School of Civil and Environmental Engineering and School of Earth and Atmospheric Sciences, Georgia Institute of Technology, Atlanta, Georgia, USA.

0094-8276/06/2006GL026816$05.00

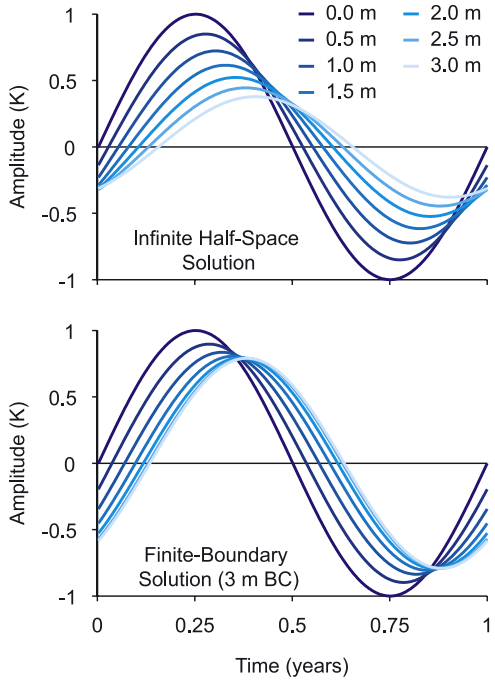

Figure 1. Two solutions to the one-dimensional diffusion equation. (top) Temperatures as a function of depth for an infinite half space forced at its surface by a temperature sinusoid of annual period and zero mean. (bottom) Solutions for a slab of finite thickness, again with a surface boundary condition equal to a sinusoid with annual period and zero mean, and with a zero-flux lower boundary condition (BC) set at 3 m.

boundary condition of unit amplitude and zero mean, the steady-state solution of the one-dimensional thermal diffusion equation takes the form (see *Carslaw and Jaeger* [1959] for an extensive discussion on both of the solutions presented here):

$$T(z,t) = A\sin\left(\frac{2\pi t}{\tau} + \varepsilon - \phi\right) \tag{1}$$

where t is time, τ is the period of the oscillation, and ε is the initial phase of the oscillation. The amplitude (A) and the phase shift (ϕ) of the downward propagating thermal wave are dependent on depth (z), the period of the surface sinusoid, and the thermophysical properties of the subsurface. In the case of the first scenario, the infinite half-space (IHS) solution, A and ϕ take the forms:

$$A_{IHS} = e^{-kz} \tag{2}$$

and

$$\phi_{IHS} = kz. \tag{3}$$

The wave vector k is defined as:

$$k = \left(\frac{\pi}{\tau\kappa}\right)^{1/2}. \tag{4}$$

For the second scenario, the finite-boundary (FB) solution, A and ϕ are also dependent on the depth of the lower boundary, l, and take the forms:

$$A_{FB} = \left(\frac{\cosh[2(l-z)k] + \cos[2(l-z)k]}{\cosh[2lk] + \cos[2lk]}\right)^{1/2} \tag{5}$$

and

$$\phi_{FB} = -\arg\left(\frac{\cosh[k(l-z)(1+i)]}{\cosh[kl(1+i)]}\right). \tag{6}$$

The differences in the two solutions arise because the FB solution must satisfy both the upper and lower boundary conditions. As l tends to infinity, the FB solution converges to the IHS solution. For shallow depths (small values of l), however, the two solutions are quite different.

[7] The IHS and FB solutions are plotted in Figure 1; a visual inspection of the two solutions reveals clear differences. Both solutions are determined for a sinusoidal surface temperature boundary condition with unit amplitude, zero mean and annual period. The subsurface thermal diffusivity in each case is set equal to 1×10^{-6} m^2 s^{-1}, a value typical for most common crustal rocks [e.g., *Carslaw and Jaeger*, 1959]. The lower boundary is at 3 m depth in the FB solution, a typical depth used in land-surface schemes of General Circulation Models (GCMs) (see Section 4 for a discussion). In Figure 2a we plot the percent amplitude attenuation of the annual signal for both scenarios, that is, the difference between 100% and the percent ratio between the surface and subsurface temperature amplitudes. The FB scenario yields temperature oscillations that are much less attenuated with depth – at 3 m the FB solution is attenuated only 21%, while the IHS solution is more than 62% attenuated. In Figure 2b we plot the phase behavior of the two scenarios. The thermal oscillations of the FB solutions are lagged later in the year at most depths, relative to the IHS solution. These oscillations converge to a constant phase at lower depths and lead the IHS solution by more than 10 days at 3 m.

3. Depth and Frequency Sensitivity

[8] The influence of the zero-flux lower-boundary condition on downward propagating temperature signals is dependent on both the depth of the boundary and the frequency of the signal. High frequency oscillations with periods on the order of days are attenuated rapidly and have no significant power below approximately 50 centimeters. A lower boundary at several meters therefore plays no significant role in the propagation of these signals. Signals with longer periods, however, propagate to deeper depths and a lower boundary at several meters progressively influences the behavior of these signals. The influence of the lower boundary arises because the choice of the zero-flux condition requires the temperature gradient at the boundary to be zero. This behavior is evident in Figure 2 in which the amplitude and phases of the annual signal converge to constant values near the lower boundary.

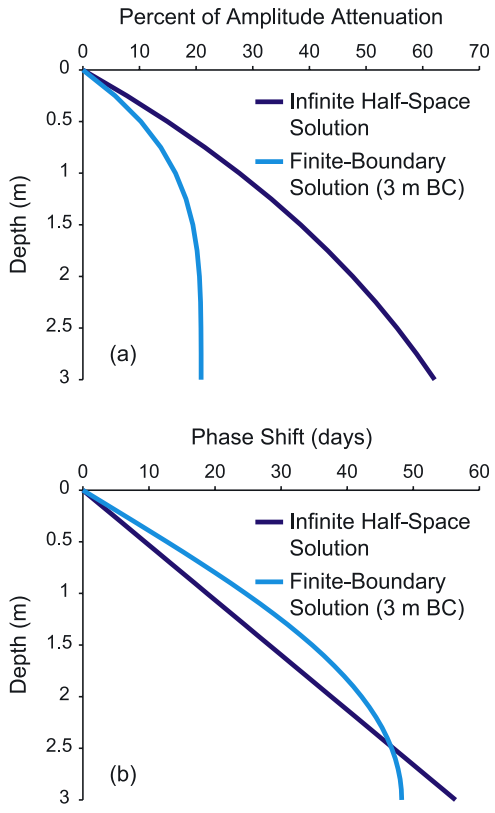

Figure 2. (a) Percent attenuation of the amplitude of an annual sinusoid in the IHS and FB solutions. Percent attenuation is calculated as the difference between 100% and the percent ratio between the surface and subsurface temperature amplitudes. Amplitude attenuation in the IHS solution is an exponential function of depth, while the FB solution is attenuated less with depth and converges to a constant amplitude by about 2.25 m. (b) Same as in Figure 2a, but for phase shifts. Phase shift is linear in the IHS solution, while the FB solution is initially phase shifted more with depth before converging to a constant phase shift by about 2.75 m. The FB solutions in both plots use a 3-m lower boundary condition (BC).

Extending this behavior to very long-period oscillations, the entire depth column maintains a temperature equal to the surface oscillation – no attenuation or phase shift of long-period oscillations occur.

[9] The percent amplitude differences between the IHS and FB solutions are plotted with depth in Figure 3; percent differences are relative to the IHS solution and the FB solutions applies a lower boundary at 3 m. Amplitude differences increase downward from the surface and demonstrate their depth dependence. We note, however, that the differences converge to zero at the surface. This behavior is a byproduct of our formulation, which uses the same surface-temperature boundary condition in each scenario. Figure 3 also illustrates the frequency dependence of the differences between the two scenarios. While there are no differences associated with the diurnal signal, the annual signal is associated with the largest differences; percent differences in longer period oscillations are reduced as periods increase. This apparent similarity between the two solutions at longer periods occurs only because there is little amplitude attenuation of long-period signals in the IHS solution by 3 m. Thus, the FB solution, which has no attenuation at low frequencies, mimics the IHS solution in the shallow subsurface. These factors combine to yield differences between the amplitudes of the two solutions that peak at a specific frequency, in this case the peak is very near the annual signal.

[10] We further explore the frequency dependence of differences between the two solutions in the top plot of Figure 4, showing the percent amplitude attenuation at 1-m depth for the IHS and FB solutions (lower-boundary depths from 2 to 20 m have been considered). The percent attenuation for each solution is calculated for oscillations with periods ranging from 2×10^{-3} to 1000 years. By 1 m the IHS solution yields 100% attenuation of the short-period oscillations, a fairly rapid decline in the amount of attenuation for oscillations with periods between 1×10^{-2} and 1 year, and a more modest decline in the attenuation at longer periods. This general behavior is observed for the FB solution, but at different frequencies; they diverge from the IHS solution at periods between 0.1 and 10 yrs., with maximum divergences near annual to decadal signals. These differences are reduced as the depth of the lower-boundary condition is lowered. The bottom plot of Figure 4 displays the percent differences between the two solutions. Two features in Figure 4 are prominent: 1) depending on the location of the lower boundary, differences can be quite large, reaching more than 33% in the case of the 2-m finite boundary and almost 20% for the 3-m finite boundary; and 2) the differences for the 2, 3 and 4-m FB solutions peak very near the annual signal.

[11] The phase shifts for all solutions are shown in the top plot of Figure 5. All FB solutions converge to a constant phase shift at long periods, and lead the phases of the IHS solution. The differences between the two phases are illustrated in the bottom plot of Figure 5, in which maxi-

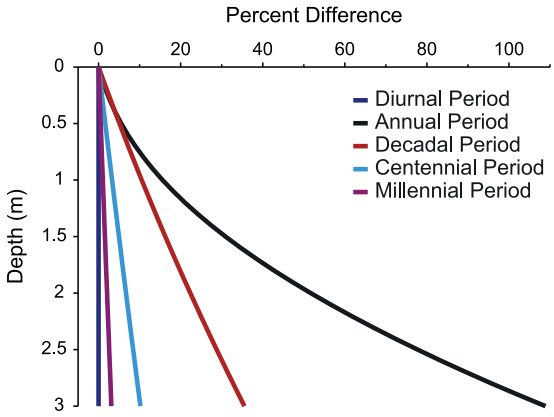

Figure 3. Percent differences (IHS vs. FB solutions) in amplitude behavior with depth for sinusoids with five different periods. The finite-boundary solution was calculated for a lower boundary at 3 m. In all cases, the near-surface layers are least affected by the boundary-condition errors, namely because the solutions each have the same surface temperature boundary conditions.

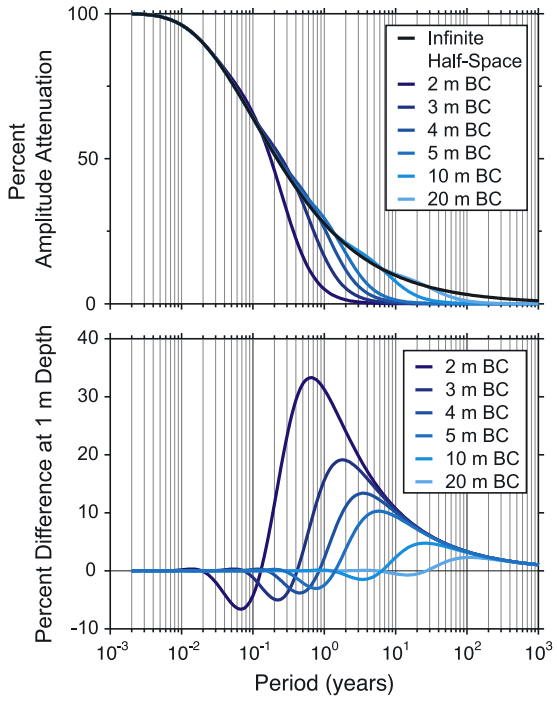

Figure 4. The amplitude behavior for the IHS solution and the FB solution with lower-boundary conditions (BC) from 2 to 20 m: (top) percent attenuation of amplitudes for each of the different solutions and (bottom) percent differences between the IHS and FB solutions. The maximum percent differences are reduced as the depth of the lower boundary is increased and the periods at which the peak differences occur become longer.

mum phase-shift differences ($100\% \times \frac{\phi_{IHS} - \phi_{FB}}{\phi_{IHS}}$, where ϕ is in units of days) tend toward 100%. The annual signal is associated with maximum negative-phase differences for lower boundaries placed at 3 and 4 m. We also note that the percent phase and amplitude differences shown in Figures 4 and 5 are for a depth of 1 m; these differences increase with depth (see Figure 3) and will be much larger below 1 m.

[12] The solutions shown in Figures 4 and 5 are also dependent on the thermal diffusivity of the subsurface. *Sun and Zhang* [2004] investigate this dependency in the context of wet or dry soils and show the effects of the lower boundary on an annual signal to increase with soil wetness, that is, increased thermal diffusivity. Interestingly, changes in the diffusivity do not change the maximum and minimum percent differences shown in Figures 4 and 5 – they shift the location of the peaks. Increased diffusivities shift the peaks toward shorter period oscillations (results not shown). The observations of *Sun and Zhang* [2004] are therefore the result of moving the peak differences shown in Figures 4 and 5 closer to the annual signal.

4. Discussion

[13] Given that the choice and location of the lower-boundary condition has been quite variable, it is hard to provide a comprehensive accounting of where and how studies have applied it. *Sun and Zhang* [2004] note a collection of modeling studies with lower boundaries that range from 1 to 6 m. They also note one study that applied a lower boundary condition at 10 m [*Stieglitz et al.*, 2001], a list to which we add two additional GCM studies that have used a lower boundary condition as deep as 10 m [*González-Rouco et al.*, 2003, 2006]. A survey of the documentation of some widely used GCMs, namely the Community Climate System Model (CCSM3) [e.g., *Lawrence and Slater*, 2005], Geophysical Fluid Dynamics Laboratory [*Milly and Shmakin*, 2002; *Anderson et al.*, 2004], Goddard Institute for Space Studies (http://www-lsce.cea.fr/pmip/docs/gissdoc.html) and the Max-Plank Institute for Meteorology (ECHAM3) models (http://www-lsce.cea.fr/pmip/docs/echam3doc.html), finds that all have applied zero-flux boundary conditions at 3.43, 1.5–6, 3.44 and 10 m, respectively. Reanalysis models also have used the same lower-boundary conventions. The European Centre for Medium-Range Weather Forecasts reanalysis package, for instance, has been evaluated using a land-surface model with a lower boundary at 2.89 m (http://www.ecmwf.int/products/data/technical/soil/discret_soil_lay.html).

[14] Our results indicate that many of the models above have used lower-boundary depths for which frequencies of interest will be considerably affected by the zero-flux

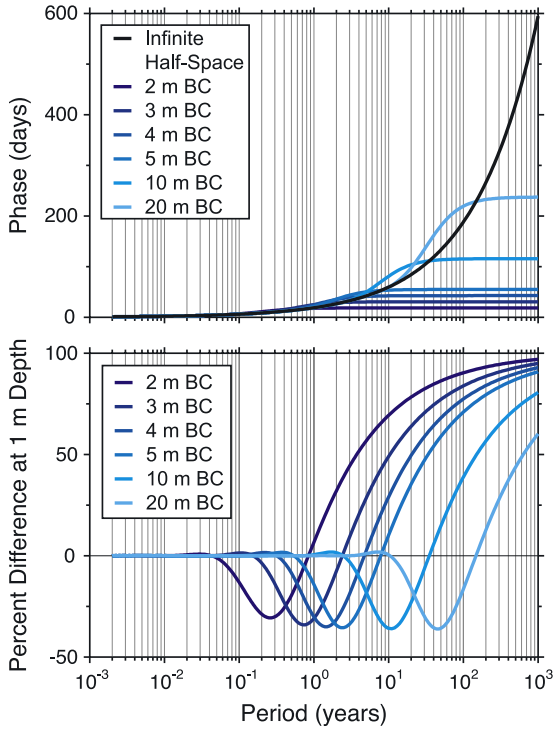

Figure 5. The phase-shift behavior for the IHS solution and the FB solution with lower-boundary conditions (BC) ranging from 2 to 20 m: (top) phase shift in days for each of the different solutions and (bottom) percent difference between the IHS and FB solutions. Unlike the amplitude behavior, the maximum percent differences in the phase shift are not reduced as the depth of the lower boundary increases, the peak differences only shift to longer periods. Nevertheless, peak negative differences are near the annual period for a lower boundary between 2 and 4 m.

condition. The corruption of subsurface temperature evolution caused by this boundary condition will impact simulations of subsurface phenomena. These phenomena include soil microbial activity, vegetation changes, hydrologic systems at high latitudes, freeze/thaw cycles, and permafrost evolution. Thus, there is a great potential for the demonstrated effects to have significant implications for many modeling studies that are tied to simulations of subsurface thermodynamics. The simple solution to the problems presented herein is to increase the depth of the lower boundary. For example, *Oelke and Zhang* [2004] and *Zhang et al.* [2005] use one-dimensional land-surface models with lower boundaries below 30 m and apply a flux condition that approximates the geothermal heat flux at the depth (these models were not used in conjunction with a GCM). Increasing the depth of the lower boundary of course increases computational costs. These costs include the length of the spin-up period required to reach equilibrium and the additional computations at the added depths. It therefore may not be feasible to increase the depth of the lower boundary ever deeper, in which case alternative boundary conditions may be more beneficial. *Lynch-Stieglitz* [1994], for instance, proposed a temperature boundary condition that approximated the amplitude and phase of the annual signal at the lower-boundary depth. Such alternatives may represent better solutions to the problems that have been outlined in this manuscript.

[15] Sensible heat storage is also relevant to many atmospheric processes on both long and short timescales. The amount of heat gained by the continental subsurface and the atmosphere during the latter half of the 20th century has been shown to be commensurate, the ground heat gain being approximately 7 to 9×10^{21} J [*Levitus et al.*, 2001, 2005; *Beltrami*, 2002; *Beltrami et al.*, 2002, 2006; *Huang*, 2006]. It is unclear, however, how the effects associated with the finite-boundary formulation may impact atmospheric simulations. Given that most land-surface models used in conjunction with GCMs have applied the lower boundary at 2–4 m, it is unlikely that many high-frequency (diurnal) signals are affected. Many of the largest effects that we have reported for boundaries between 2–4 m have been associated with intermediate frequencies of annual to decadal scale. Nevertheless, it remains to be seen whether the magnitude of the reported effects will have any consequence for atmospheric simulations, given the much larger influence of ocean heat storage at these timescales [see, e.g., *Dickinson*, 2000]. For low-frequency oscillations of centuries or more it is also unclear how our results may affect atmospheric simulations. At these low frequencies, the ground heat storage will be affected more than the absolute temperature effects there were investigated herein. Nevertheless, the magnitude of errors associated with ground heat storage will likely be small compared to ocean heat gains over the same periods [*Levitus et al.*, 2005].

5. Conclusions

[16] This study provides an assessment of the sensitivity of subsurface sensible heat calculations to the depth of a finite lower boundary. Results confirm earlier assessments by *Lynch-Stieglitz* [1994] and *Sun and Zhang* [2004], but go further by providing both a theoretical basis for the lower-boundary condition effect and an assessment over a much larger frequency range. This is particularly important because it allows differences to be evaluated against the relevant timescales of simulation, a crucial point of consideration. While *Sun and Zhang* [2004] estimated that lower boundaries should be located between 6 and 15 m, this estimate was based only on a consideration of annual signals. Simulations that employ land-surface models may require fidelity at frequencies with periods that are longer or shorter than a year. Thus, there is no single depth at which all simulations should place the lower boundary. A weather model may only require accurate simulations over a time span of several weeks, making a 2-m lower boundary more than sufficient. By contrast, climate simulations with GCMs span decades, centuries or millennia and it is not sufficient to consider only diurnal or annual time scales. Given a timescale of interest, the type of analysis presented here therefore is useful for estimating the required depth of the lower boundary.

[17] **Acknowledgments.** We thank Henry Pollack for insightful discussions on an early draft of this manuscript and Rob Harris and Hugo Beltrami for their helpful reviews. This research was supported in part by NSF grants from the Office of Polar Programs (OPP-0436118), the division of Environmental Biology (Arctic LTER Project), and a Biocomplexity Award (ATM-0439620), as well as by the NASA Seasonal-to-Interannual Prediction Project at Goddard Space Flight Center, NASA's Global Modeling and Analysis Program RTOP 622-24-47. J. E. Smerdon was additionally supported by a Lamont-Doherty Postdoctoral Fellowship from the Lamont-Doherty Earth Observatory of Columbia University.

References

Anderson, J. L., et al. (2004), The new GFDL global atmosphere and land model AM2-LM2: Evaluation with prescribed SST simulations, *J. Clim.*, *17*, 4641–4673.

Beltrami, H. (2002), Climate from borehole data: Energy fluxes and temperatures since 1500, *Geophys. Res. Lett.*, *29*(23), 2111, doi:10.1029/2002GL015702.

Beltrami, H., J. E. Smerdon, H. N. Pollack, and S. Huang (2002), Continental heat gain in the global climate system, *Geophys. Res. Lett.*, *29*(8), 1167, doi:10.1029/2001GL014310.

Beltrami, H., E. Bourlon, L. Kellman, and J. F. González-Rouco (2006), Spatial patterns of ground heat gain in the Northern Hemisphere, *Geophys. Res. Lett.*, *33*, L06717, doi:10.1029/2006GL025676.

Carslaw, H. S., and J. C. Jaeger (1959), *Conduction of Heat in Solids*, 2nd ed., 510 pp., Oxford Univ. Press, New York.

Dickinson, R. E. (2000), How coupling of the atmosphere to ocean and land helps determine the timescales of interannual variability of climate, *J. Geophys. Res.*, *105*(D15), 20,115–20,120.

González-Rouco, F., H. von Storch, and E. Zorita (2003), Deep soil temperature as proxy for surface air-temperature in a coupled model simulation of the last thousand years, *Geophys. Res. Lett.*, *30*(21), 2116, doi:10.1029/2003GL018264.

González-Rouco, J. F., H. Beltrami, E. Zorita, and H. von Storch (2006), Simulation and inversion of borehole temperature profiles in surrogate climates: Spatial distribution and surface coupling, *Geophys. Res. Lett.*, *33*, L01703, doi:10.1029/2005GL024693.

Hillel, D. (1998), *Environmental Soil Physics*, 771 pp., Elsevier, New York.

Huang, S. (2006), 1851–2004 annual heat budget of the continental landmasses, *Geophys. Res. Lett.*, *33*, L04707, doi:10.1029/2005GL025300.

Lawrence, D. M., and A. G. Slater (2005), A projection of severe near-surface permafrost degradation during the 21st century, *Geophys. Res. Lett.*, *32*, L24401, doi:10.1029/2005GL025080.

Levitus, S., J. Antonov, J. Wang, T. L. Delworth, K. Dixon, and A. Broccoli (2001), Anthropogenic warming of the Earth's climate system, *Science*, *292*, 267–270.

Levitus, S., J. Antonov, and T. Boyer (2005), Warming of the world ocean, 1955–2003, *Geophys. Res. Lett.*, *32*, L02604, doi:10.1029/2004GL021592.

Lynch-Stieglitz, M. (1994), The development and validation of a simple snow model for the GISS GCM, *J. Clim.*, *7*, 1842–1855.

Milly, P. C. D., and A. B. Shmakin (2002), Global modeling of land water and energy balances. part I: The land dynamics (LaD) model, *J. Hydrometeorol.*, *3*, 283–299.

Oelke, C., and T. Zhang (2004), A model study of circum-Arctic soil temperatures, *Permafrost Periglacial Processes*, *15*, 103–121.

Schulz, J.-P., L. Dumenil, J. Polcher, C. A. Schlosser, and Y. Xue (1998), Land surface energy and moisture fluxes: Comparing three models, *J. Appl. Meteorol.*, *37*, 288–307.

Stieglitz, M., A. Ducharne, R. Koster, and M. Suarez (2001), The impact of detailed snow physics on the simulation of snow cover and subsurface thermodynamics at continental scales, *J. Hydrometeorol.*, *2*, 228–242.

Sun, S., and X. Zhang (2004), Effect of the lower boundary position of the Fourier equation on the soil energy balance, *Adv. Atmos. Sci.*, *21*, 868–878.

Zhang, Y., W. Chen, S. L. Smith, D. W. Riseborough, and J. Cihlar (2005), Soil temperature in Canada during the twentieth century: Complex responses to atmospheric climate change, *J. Geophys. Res.*, *110*, D03112, doi:10.1029/2004JD004910.

J. E. Smerdon, Lamont-Doherty Earth Observatory, Columbia University, Palisades, NY 10964, USA. (jsmerdon@ldeo.columbia.edu)

M. Stieglitz, School of Civil and Environmental Engineering and School of Earth and Atmospheric Sciences, Georgia Institute of Technology, Atlanta, GA 30332, USA.